Supporting Information

Multi-modal imaging probe for glypican-3 overexpressed in orthotopic hepatocellular carcinoma

Shuo Feng,[1§] Xiaoqing Meng,[1§] Zhao Li,[5§] Tse-Shao Chang,[2] Xiaoli Wu,[1] Juan Zhou,[1] Bishnu Joshi,[1] Eun-Young Choi,[3] Lili Zhao,[4] Jiye Zhu,[5*] and Thomas D. Wang[1,2,6*]

[1]Department of Medicine, Division of Gastroenterology, University of Michigan, Ann Arbor, MI 48109

[2]Department of Mechanical Engineering, University of Michigan, Ann Arbor, Michigan 48109

[3]Department of Pathology, University of Michigan, Ann Arbor, Michigan 48109

[4]Department of Biostatistics, University of Michigan, Ann Arbor, Michigan 48109

[5]Department of Hepatobiliary Surgery, Peking University People's Hospital, Beijing, China

[6]Department of Biomedical Engineering, University of Michigan, Ann Arbor, Michigan 48109

[§]Authors contributed equally

***Corresponding author**:

Jiye Zhu, Ph.D.
Professor of Department of Hepatobiliary Surgery
Peking University People's Hospital,
Beijing, 100044
Office: (8610)88324176
Fax: (8610)88324175
Email: moc.anis.piv@kwnadnag

Thomas D. Wang, M.D., Ph.D.

Professor of Medicine, Biomedical Engineering, and Mechanical Engineering
H. Marvin Pollard Collegiate Professor of Endoscopy Research
Division of Gastroenterology, University of Michigan
109 Zina Pitcher Pl. BSRB 1522
Ann Arbor, MI 48109-2200
Office: (734) 936-1228
Fax: (734) 647-7950
Email: thomaswa@umich.edu

Table of contents:

Gene	A GSE14520 *P*-value	fold-Δ	B GSE44074 *P*-value	fold-Δ
CCT3	6.9E-85	3.0	8.4E-08	1.8
CAP2	1.2E-82	6.0	8.1E-02	1.2
ACLY	1.0E-80	3.1	3.5E-09	1.6
PRC1	4.7E-80	5.5	#N/A	#N/A
GPC3	1.1E-70	29.3	3.5E-15	4.4
IRAK1	1.8E-68	2.5	3.4E-02	1.3
ENAH	7.2E-68	3.9	#N/A	#N/A
HSPB1	2.3E-67	2.9	1.5E-02	1.4
HSP90AB1	6.2E-63	2.3	#N/A	#N/A
ROBO1	4.8E-62	6.8	2.7E-05	1.3
ITGA6	3.0E-61	2.8	4.9E-02	1.3

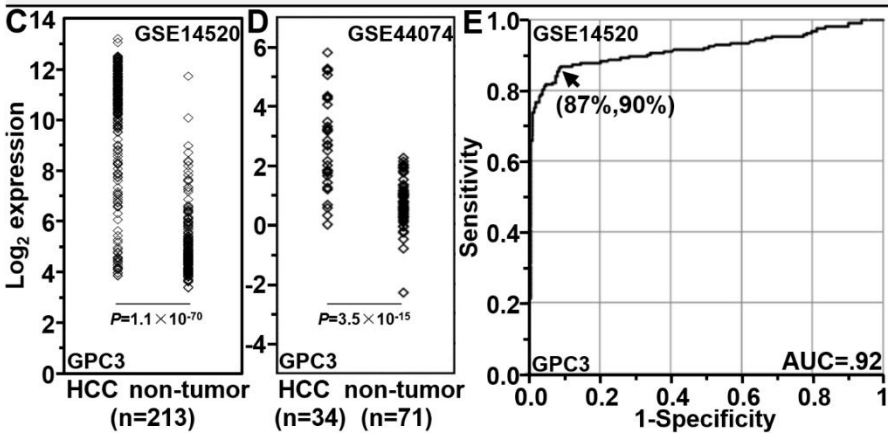

Fig. **S1** – **Tissue target for HCC**. **A**,**B)** Gene expression profiles from GSE14520 and GSE44074 were sorted by gene ontology (GO) term for cell membrane. GPC3 showed the highest average fold-change (Δ) in both datasets. Log-transformed data for expression of GPC3 in HCC and non-tumor was plotted for **C**) GSE14520 and **D**) GSE44074. **E**) ROC curve for GSE14520 shows an area-under-the curve (AUC) of 0.92 with 87% sensitivity and 90% specificity.

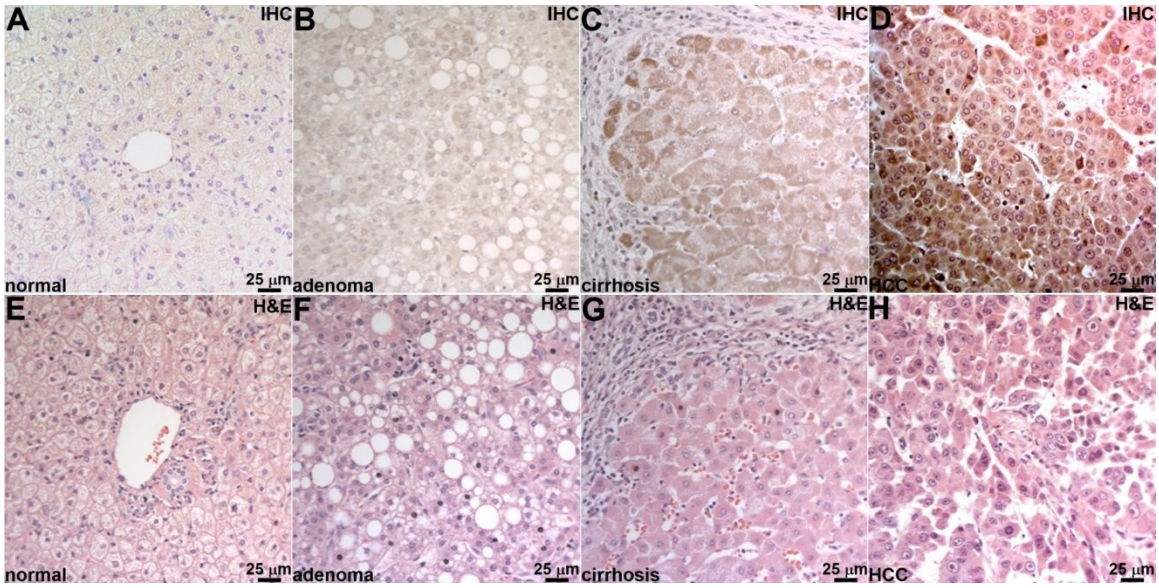

Fig. **S2** – **Validation by immunohistochemistry**. Representative sections of **A**) normal liver, **B**) adenoma, and **C**) cirrhosis showed minimal anti-GPC3 reactivity by comparison with **D**) HCC. Strong (3+) and moderate (2+) staining was found in n=16 and 6 specimens, respectively, resulting in a total of 22/25 (88%) positives. **E**-**H**) Histology (H&E) from adjacent sections is shown.

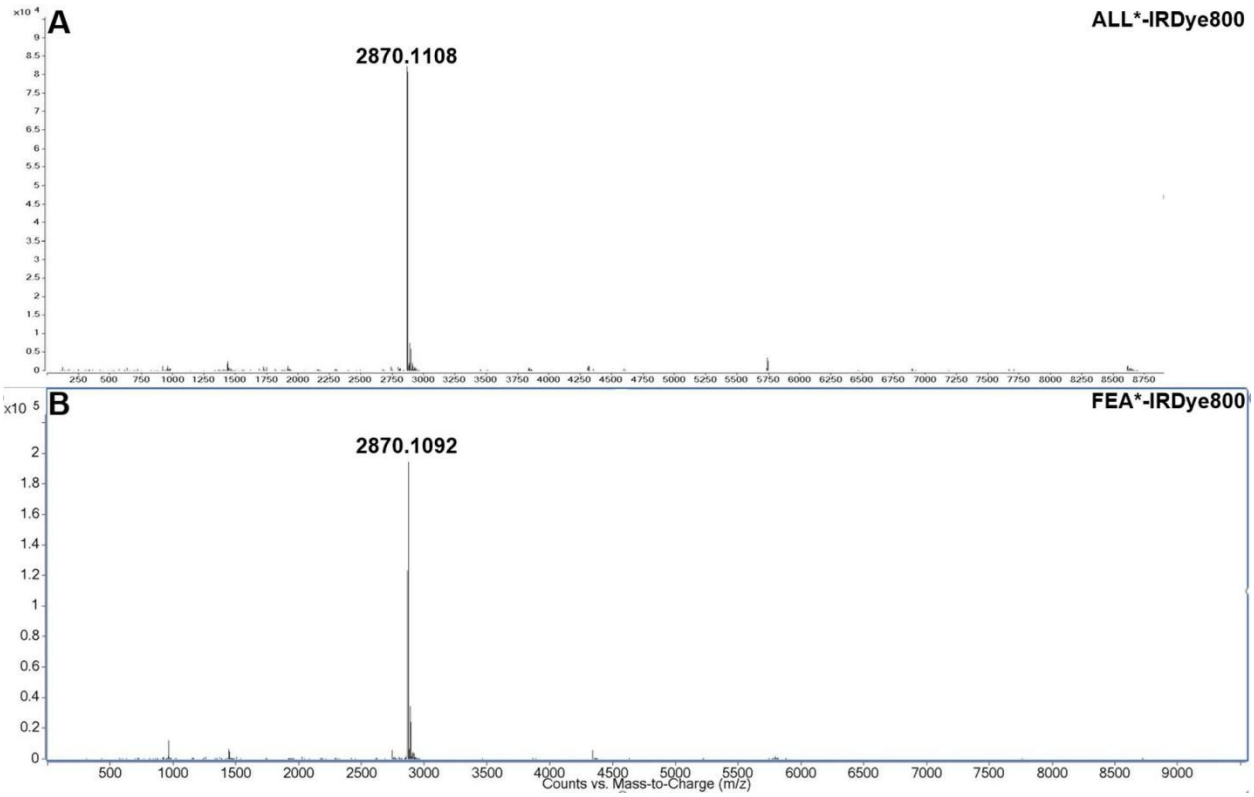

Fig. **S3** – **Mass spectrometry**. A mass-to-charge (m/z) ratio of 2870.11 and 2870.11 was measured for **A**) ALL*-IRDye800 and **B**) FEA*-IRDye800, respectively, which agrees with the expected value of 2870.09 for either peptide.

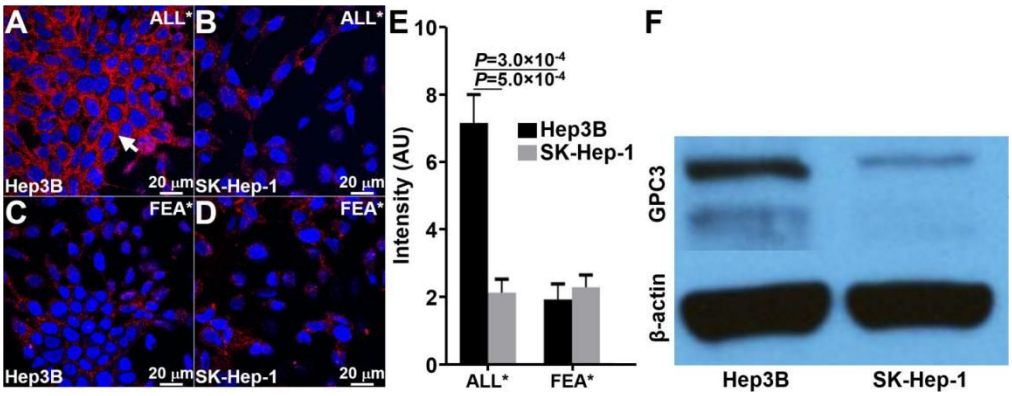

Fig. S4 – **Specific peptide binding to GPC3**. ALL*-IRDye800 shows strong binding with **A**) Hep3B cells and minimal binding with **B**) SK-Hep-1 cells in vitro. FEA*-IRDye800 shows minimal binding with **C**) Hep3B cells and **D**) SK-Hep-1 cells. **E**) Quantified fluorescence intensities. The mean fluorescence intensities for ALL*-IRDye800 with Hep3B cells was significantly greater than that with SK-Hep-1 cells with 3.3-fold increase . The mean fluorescence intensities for ALL*-IRDye800 was significantly greater than FEA*-IRDye800 with SK-Hep-1 cells with 3.7-fold increase. The P-values were determined using a one-way ANOVA. **F**) Western blot shows GPC3 expression for the cell lines.

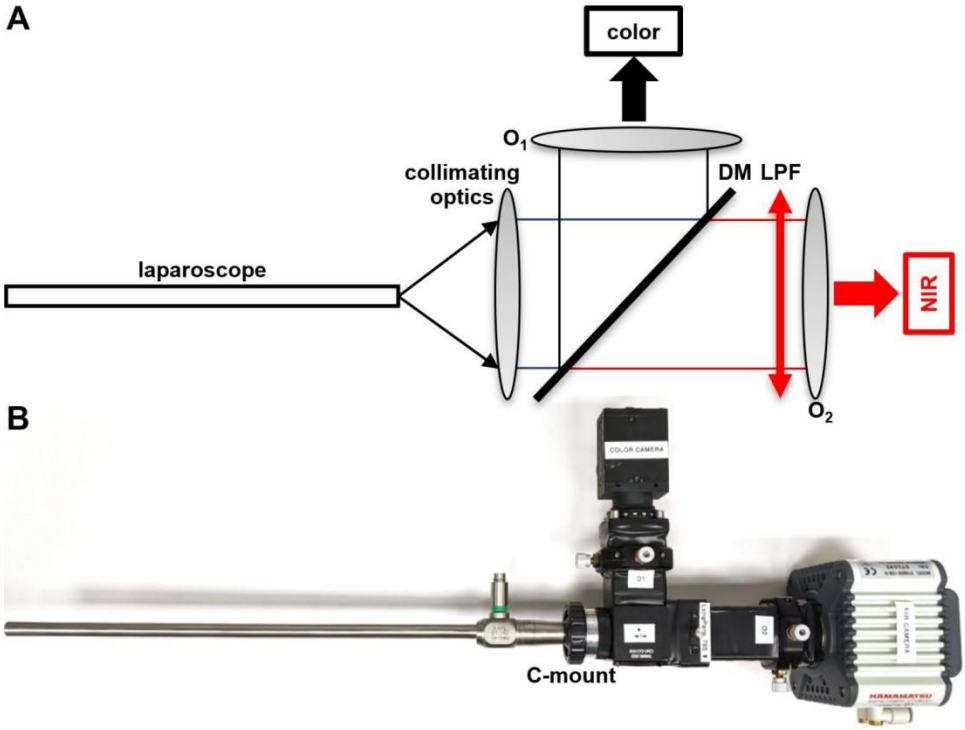

Fig. **S5** – **NIR laparoscope**. **A**) Light collected by a standard surgical laparoscope (#49003 AA, Karl Storz) is collimated. Reflectance is deflected by a dichroic mirror (DM, #Di02-R785-25x36, Semrock). Focusing optics O_1 (#49-766, Edmund Optics) converges the reflectance beam onto a color camera (#GX-FW-28S5C-C, Point Grey Research). NIR fluorescence passes through a long pass filter (LPF, #BLP01-785R-25, Semrock) and is focused by objective O_2 (#49-792-INK, Edmund Optics) onto a sensitive NIR fluorescence camera (Orca R-2, Hamamatsu Photonic). White light illumination (MCWHL5, Thorlabs) and laser excitation at λ_{ex} = 785 nm (#iBEAM-SMART-785-S, Toptica Photonics) are coupled via a liquid light guide (LLG3-4Z, Thorlabs) into the laparoscope. **B**) Photo shows the imaging module attached to laparoscope via a standard C-mount connector.

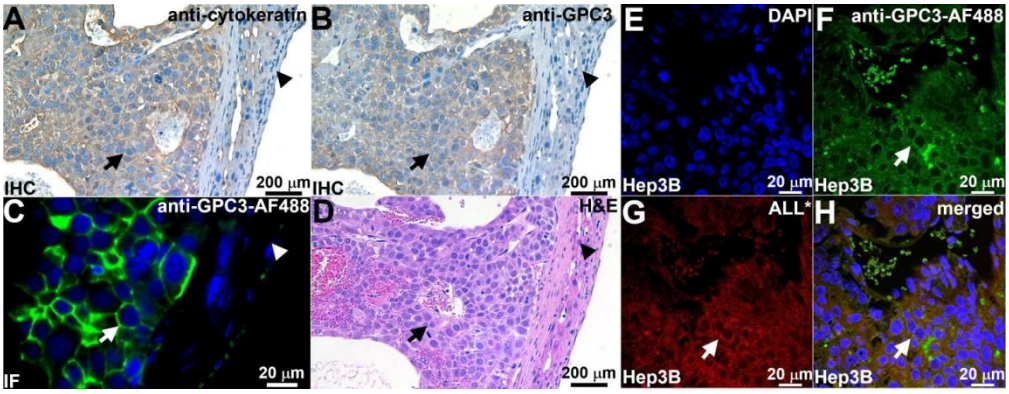

Fig. **S6** – **Specific binding to orthotopic xenograft HCC tumor ex vivo**. **A**) Increased anti-cytokeratin reactivity shows presence of human HCC tumor (arrow) imbedded in mouse liver (arrowhead). **B**) Strong anti-GPC3 staining (arrow) confirms GPC3 expression in HCC. **C**) Bright fluorescence is seen on cell surface (arrow) in HCC. **D**) Corresponding histology (H&E) shows presence of human HCC tumor (arrow) implanted in mouse liver (arrowhead). On immunofluorescence, **E**) DAPI, **F**) anti-GPC3-AF488 (green) and **G**) ALL*-IRDye800 (red) show staining to the cell surface (arrows) in orthotopic xenograft HCC tumor. A Pearson's correlation coefficient of $\rho = 0.70$ was calculated from the **H**) merged image.

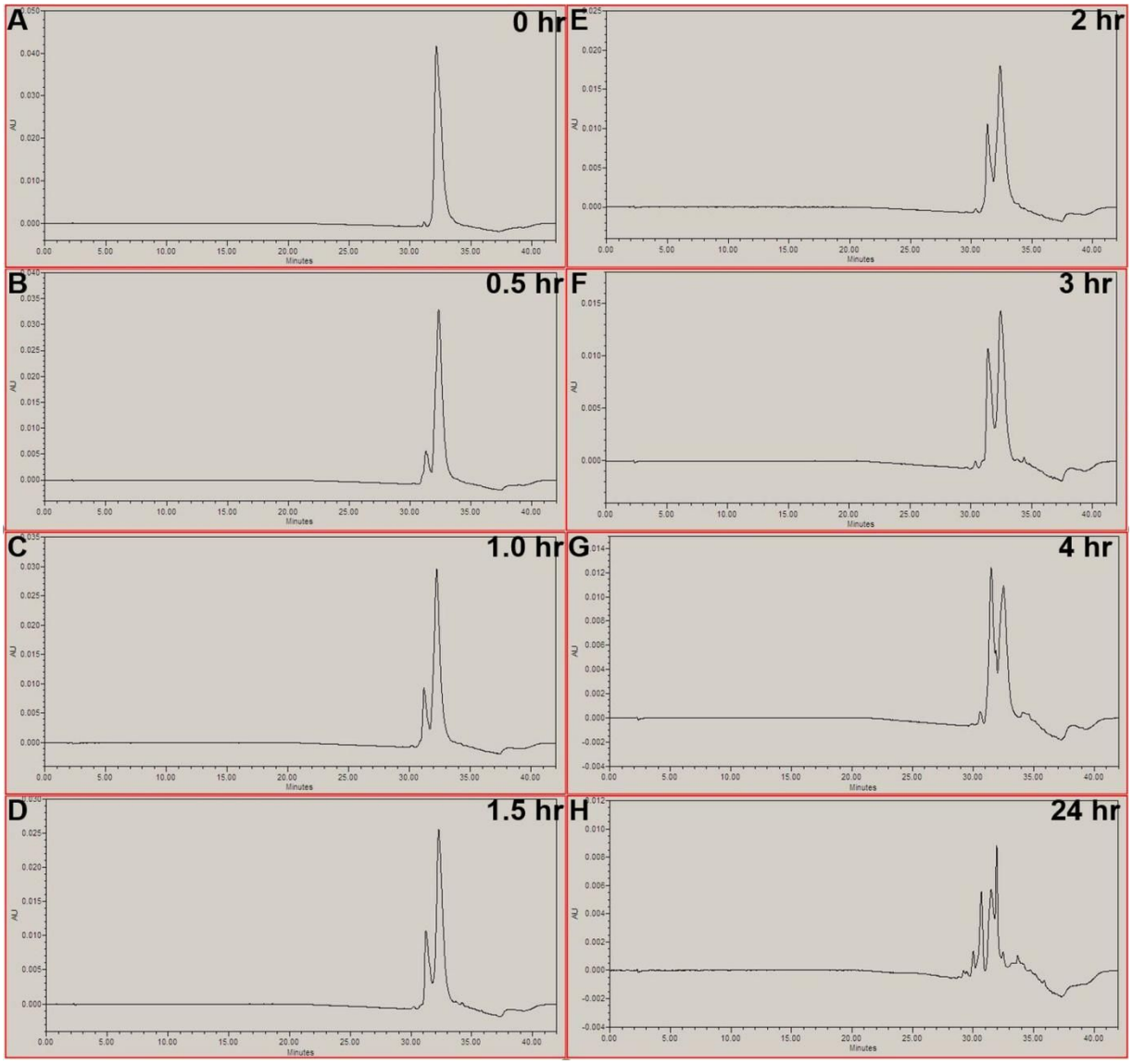

Fig. **S7** – **Serum stability**. ALL*-IRDye800 incubated in mouse serum were measured with HPLC at **A**-**H**) 0, 0.5, 1.0, 1.5, 2, 3, 4, and 24 hours.

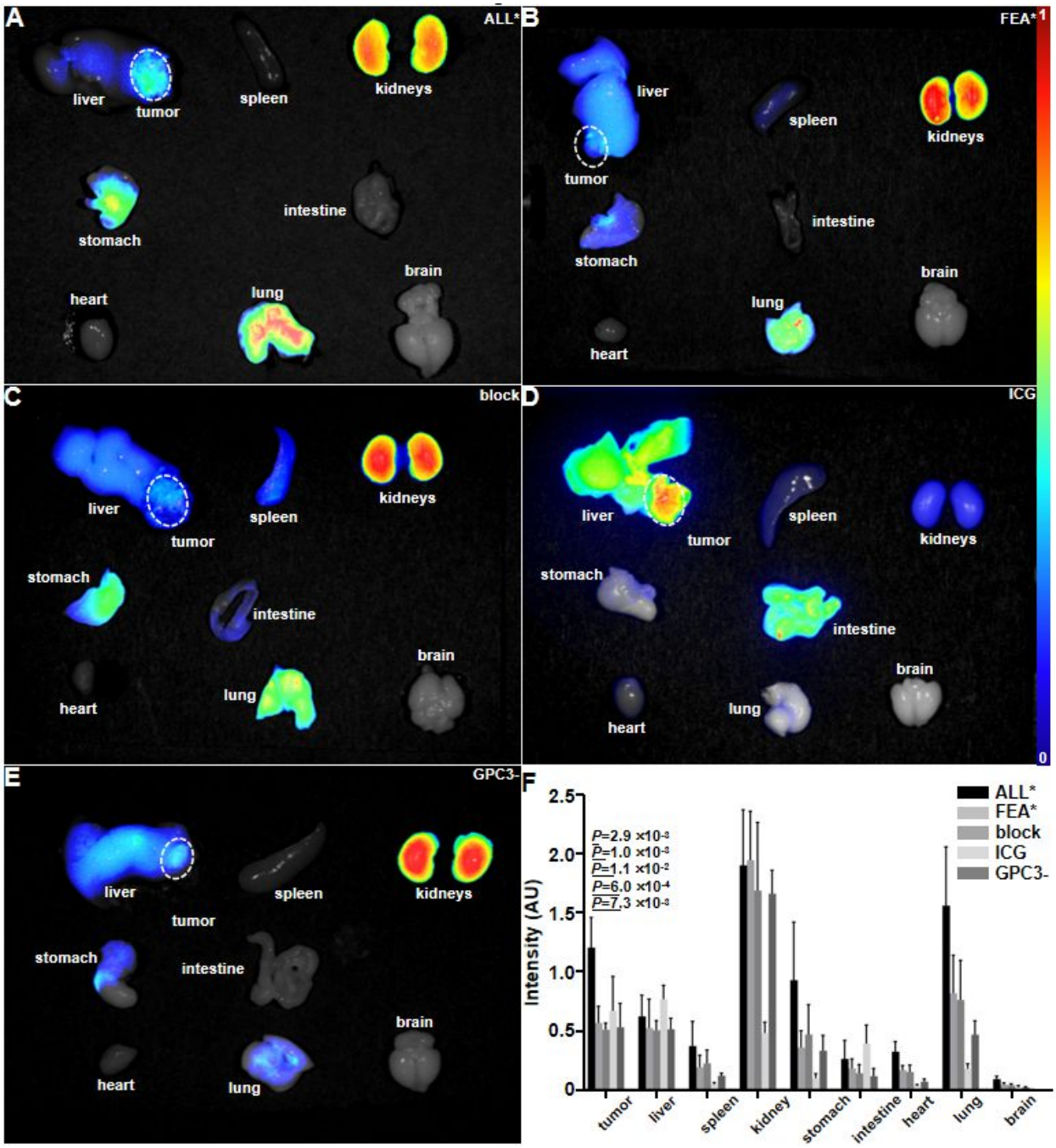

Fig. **S8** – **Peptide biodistribution**. Representative fluorescence images are shown from major organs excised from mice bearing HCC xenograft tumors. The mice were euthanized 1.5 hours after intravenous injection of **A**) ALL*-IRDye800, **B**) FEA*-IRDye800, **C**) ALL* (block), **D**) ICG and **E**) GPC3- with n = 5 animals per group. **F**) Quantified results show that the mean (±SD) intensity from tumor was significantly higher for ALL*-IRDye800 versus FEA*-IRDye800, ALL* (block), ICG and GPC3- with a 2.1 and 2.4, 1.8 and 2.3-fold increase, respectively. The result for ALL*-IRDye800 was greater in tumor than adjacent normal liver with a 1.9-fold increase. Pairwise P-values were calculated from ANOVA model with Dunnett adjustment for multiple comparisons.

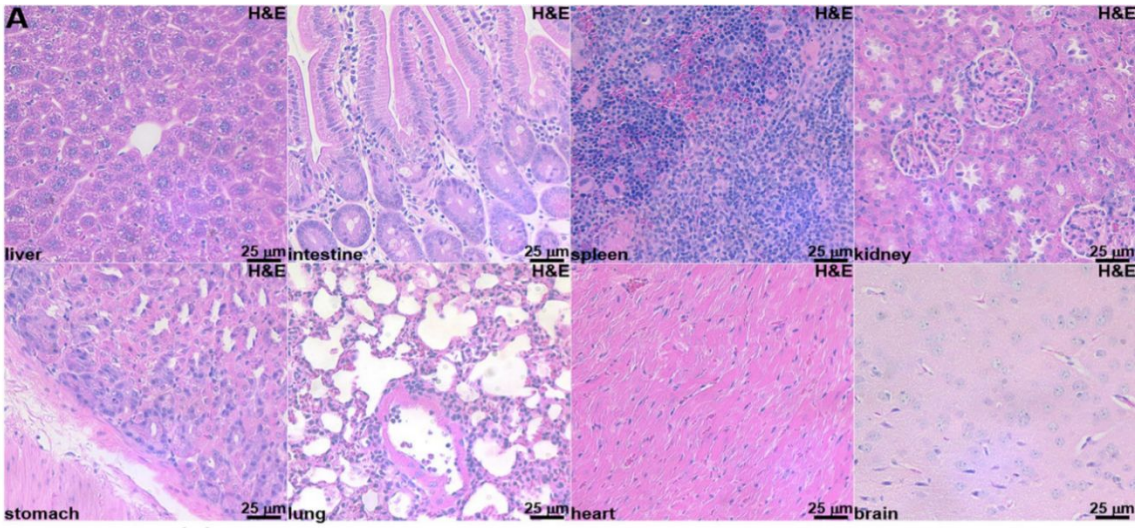

B

Lab	Unit	PBS	ALL*-IRDye800	Ref
White blood cells (WBC)	10^3/μL	4.80±0.55	4.49±2.24	0.80–10.60
Neutrophils (NEU)	10^3/μL	0.70±0.04	0.53±0.18	0.23–3.60
Lymphocytes (LYM)	10^3/μL	3.89±0.55	3.70±2.03	0.60–8.90
Monocytes (MONO)	10^3/μL	0.12±0.03	0.09±0.01	0.04–1.40
Eosinophils (EOS)	10^3/μL	0.07±0.02	0.13±0.03	0.00–0.51
Basophils (BAS)	10^3/μL	0.01±0.00	0.03±0.02	0.00–0.12
NEU %	%	14.70±1.87	12.70±1.73	6.5– 50.0
LYM %	%	80.87±2.31	80.13±3.98	40.0–92.0
MONO %	%	2.57±0.36	2.70±1.07	0.9–18.0
EOS %	%	1.63±0.71	3.50±1.33	0.0–7.5
BAS %	%	0.23±0.04	0.97±0.56	0.0–1.5
Red blood cells (RBC)	10^6/μL	9.15±0.30	8.46±0.31	6.50–11.50
Hemoglobin (HGB)	g/dL	14.87±0.58	14.13±0.38	11.0–16.5
Hematocrit (HCT)	%	42.87±1.84	40.70±0.93	35.0–55.0
Mean corpuscular (MCV)	fL	46.87±0.56	48.17±0.71	41.0–55.0
Cell hemoglobin (MCH)	Pg	16.23±0.11	16.73±0.22	13.0–18.0
Cell hemoglobin concentration (MCHC)	g/dL	34.63±0.18	34.77±0.11	30.0–36.0
Red cell distribution width (RDW)	%	12.73±0.29	11.87±0.18	12.0–19.0
Platelets (PLT)	10^3/μL	1096.67±128.89	624.67±317.11	400–1600
Mean platelet volume (MPV)	fL	4.80±0.00	5.00±0.13	4.0–6.2

C

Lab	Units	PBS	ALL*-IRDye800	Ref
AST	U/L	99±18	104±15.5	39.55-386.05
ALT	U/L	81±14	92±13	24.30-115.25
ALP	U/L	147.7±15.1	135.2±14.8	65.50-364.20
TBIL	mg/dL	0.19±0.06	0.1±0.01	0.12-0.58
BUN	mg/dL	24.3±3.6	25.5±1.5	5.15-30.70
Cr	mg/dL	0.27±0.03	0.22±0.03	0.09-0.40
Alb	g/dL	3.33±0.31	2.98±0.088	2.72-4.20

Fig. **S9** – **Animal necropsy**. **A**) Normal healthy mice were sacrificed 48 hours post-injection with ALL*-IRDye800. No signs of acute toxicity were seen on histology (H&E) of vital organs, including liver, intestine, spleen, kidney, stomach, lung, heart, and brain, and from **B**) Hematology test. Results from n = 3 mice are shown. **C**) Serum chemistries. Results from n = 3 mice are shown.

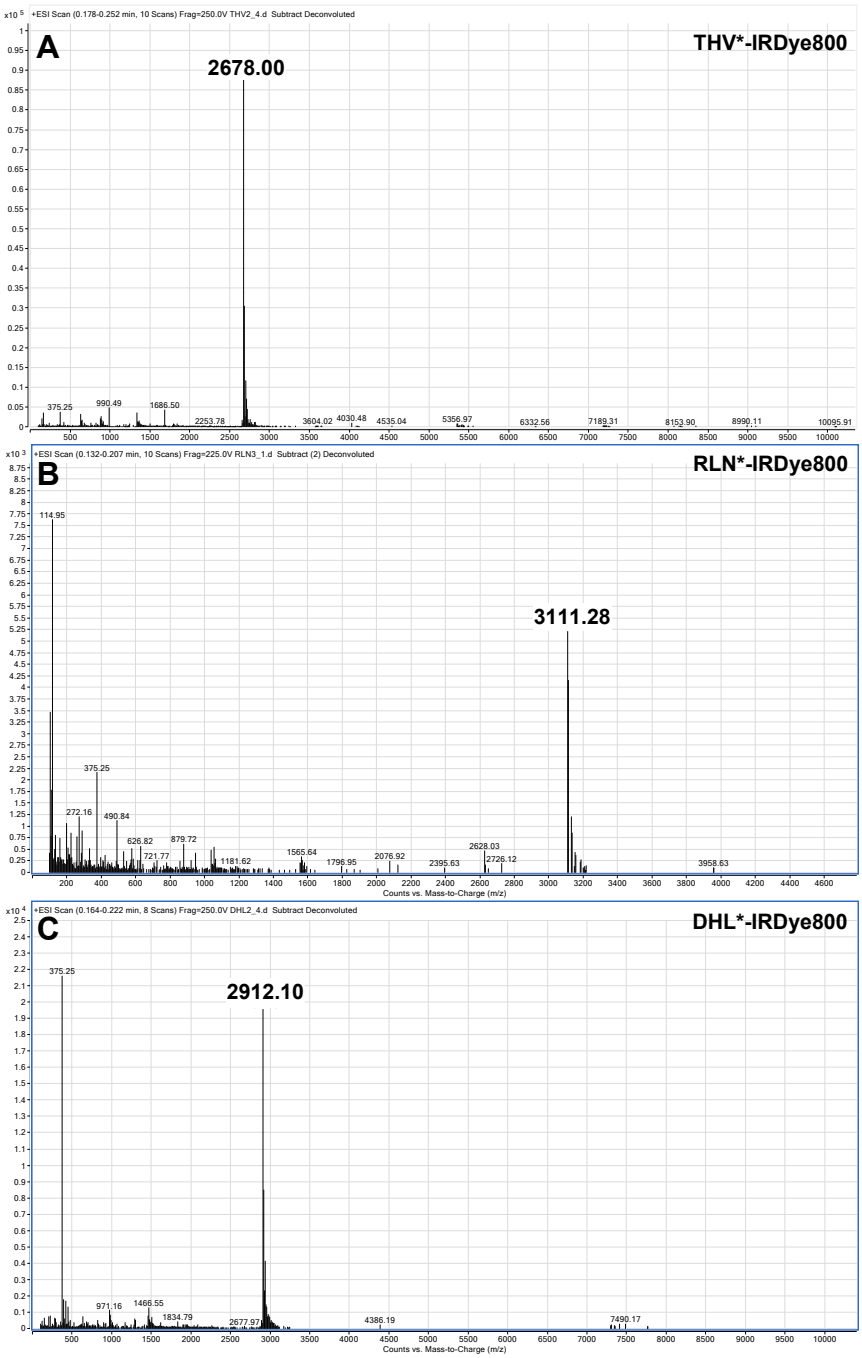

Fig. **S10 – Mass spectrometry of reported peptides**. A mass-to-charge (m/z) ratio of 2678.00, 3111.28 and 2912.10 was measured for **A**) THV*-IRDye800, **B**) RLN*-IRDye800 and **C**) DHL*-IRDye800, respectively, which agrees with the expected value of 2678.00, 3111.29 and 2912.11 for either peptide.

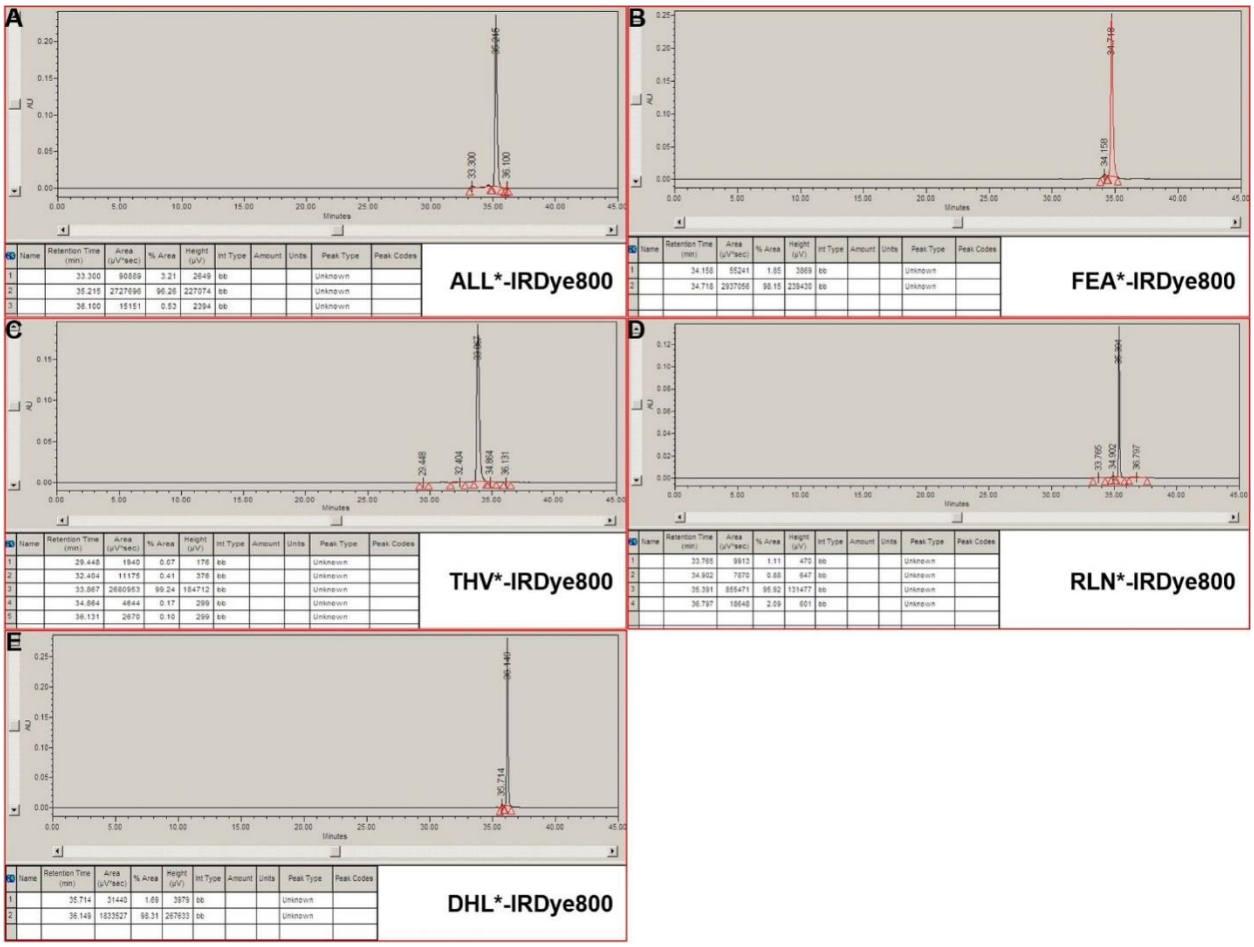

Fig. **S11** – **Peptide purity measured by RP-HPLC**. **A**) ALL*-IRDye800, **B**) FEA*-IRDye800, **C**) THV*-IRDye800, **D**) RLN*-IRDye800, and **E**) DHL*-IRDye800 were found to have purity of 96.26%, 98.15%, 99.24%, 95.92%, and 98.15%, respectively.

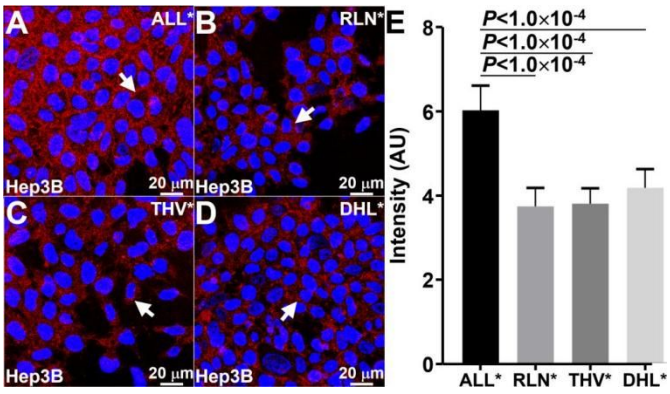

Fig. **S12** – **Peptide binding comparison to GPC3 in vitro**. **A**) ALL*-IRDye800, **B**) RLN*-IRDye800, **C**) THV*-IRDye800, and **D**) DHL* -IRDye800 were incubated with Hep3B cells in vitro for GPC3 bind comparison. **E**) The mean fluorescence intensities for ALL*-IRDye800 was significantly greater than that for RLN*-IRDye800, THV*-IRDye800 and DHL*-IRDye800 with an incease of 1.6, 1.6 and 1.4-fold. The *P*-values were determined using a one-way ANOVA.